2396–2405 *Nucleic Acids Research, 2000, Vol. 28, No. 12*

Characterization of the human and mouse WRN 3′→5′ exonuclease

Shurong Huang, Sergey Beresten[1], Baomin Li, Junko Oshima[2], Nathan A. Ellis[1] and Judith Campisi*

Life Sciences Division, Mailstop 84-144, Lawrence Berkeley National Laboratory, 1 Cyclotron Road, Berkeley, CA 94720, USA, [1]Department of Human Genetics, Laboratory of Cancer Susceptibility, Memorial Sloan-Kettering Cancer Center, New York, NY 10021, USA and [2]Department of Pathology, University of Washington, Seattle, WA 98195, USA

Received February 2, 2000; Revised and Accepted May 2, 2000

ABSTRACT

Werner's syndrome (WS) is an autosomal recessive disorder in humans characterized by the premature development of a partial array of age-associated pathologies. *WRN*, the gene defective in WS, encodes a 1432 amino acid protein (hWRN) with intrinsic 3′→5′ DNA helicase activity. We recently showed that hWRN is also a 3′→5′ exonuclease. Here, we further characterize the hWRN exonuclease. hWRN efficiently degraded the 3′ recessed strands of double-stranded DNA or a DNA–RNA heteroduplex. It had little or no activity on blunt-ended DNA, DNA with a 3′ protruding strand, or single-stranded DNA. The hWRN exonuclease efficiently removed a mismatched nucleotide at a 3′ recessed terminus, and was capable of initiating DNA degradation from a 12-nt gap, or a nick. We further show that the mouse WRN (mWRN) is also a 3′→5′ exonuclease, with substrate specificity similar to that of hWRN. Finally, we show that hWRN forms a trimer and interacts with the proliferating cell nuclear antigen *in vitro*. These findings provide new data on the biochemical activities of WRN that may help elucidate its role(s) in DNA metabolism.

INTRODUCTION

Werner's syndrome (WS) is a rare autosomal recessive disorder, also referred to as a segmental premature aging syndrome or progeria of the adult (1–3). Affected individuals prematurely develop many, but not all, of the pathologies associated with old age. The clinical manifestations of WS include atherosclerosis, bilateral ocular cataracts, type II diabetes, hyperlipidemia, gonadal atrophy, osteoporosis and various types of benign and malignant neoplasms, in addition to an aged appearance. WS patients develop these age-related disorders two or three decades earlier than normal subjects and eventually succumb to either cardiovascular disease or cancer at an average age of 45 years (2,3).

Cells from individuals with WS have a short replicative life span and long S phase compared to cells from age-matched controls (4–6). In addition, the senescent phenotype of WS cells differs in selected ways from that of normal cells. WS cells senesce with longer than normal telomeres (7), and show robust c-fos inducibility (8), which does not occur in normal cells. WS cells undergo chromosome rearrangements with a relatively high frequency (9,10), display elevated rates of homologous recombination (11) and are highly sensitive to the DNA damaging agent 4-nitroquinoline-1-oxide (4NQO) (12). These cellular phenotypes suggest that mutations in the WS locus lead to defects in one or more aspect of DNA metabolism.

The gene defective in WS, *WRN*, encodes a large protein with a central region that is highly homologous to the *Escherichia coli* RECQ helicase (13). Consistent with this homology, the WRN protein was shown to have DNA helicase activity *in vitro* (14,15). WRN is now known to belong to a multigene family of RECQ-like helicases, at least three of which (*WRN*, *BLM* and *RECQL4*) are associated with hereditary disorders in humans. Mutations in *BLM* and *RECQL4* lead to phenotypes that differ in several ways from WS (16). The diverse phenotypes caused by defects in different *RECQ*-like genes may be partly due to different expression patterns (17). In addition, each RECQ-like helicase may have a distinct substrate specificity, interact with different regulatory proteins and/or contain other yet uncharacterized functions. This last possibility is supported by the identification of a motif in *WRN*, but not the other *RECQ*-like genes, that is present in many 3′→5′ exonucleases (18,19). Recently, we and others showed that WRN is indeed a 3′→5′ exonuclease (20,21). Here, we further characterize the WRN exonuclease. We show that both human and mouse WRN (hWRN and mWRN, respectively) are 3′→5′ exonucleases with similar substrate specificities. Both proteins prefer double-stranded DNA with a 3′ recessed end, can degrade DNA from a gap or nick, and efficiently remove a terminal mismatched nucleotide. In addition, we show that WRN forms a trimer *in vitro*, and confirm the finding that WRN interacts with the proliferating cell nuclear antigen (PCNA). These findings suggest that WRN may play a unique role in DNA transactions, distinct from those of the other human RECQ-like proteins.

*To whom correspondence should be addressed. Tel: +1 510 486 4416; Fax: +1 510 486 4545; Email: jcampisi@lbl.gov

MATERIALS AND METHODS

Materials

The baculovirus expression vector pFastBacHT, recombinant baculovirus generation kit and Sf9 insect cells were obtained from Gibco BRL (Gaithersburg, MD). The TALON resin and mouse pancreatic RNA were from Clontech (Palo Alto, CA). The gel filtration column and Superose 6 resin were from Bio-Rad (Hercules, CA) and Pharmacia (Piscataway, NJ), respectively.

Expression vectors

The full-length human *WRN* cDNA (13) was cloned into pFastBacHT to generate pBac-hWRN. The first 333 codons of the *WRN* cDNA were amplified by the polymerase chain reaction (PCR) and cloned into pFastBacHT to generate pBac-hN333. The point mutation E84A (Glu→Ala at amino acid 84) was introduced by site-directed PCR mutagenesis, as described (22) to generate pBac-hN333E84A. The vector expressing the N-terminal fragment (amino acids 1–328) of the mWRN was generated as follows. Mouse (BALB/c strain) pancreas poly(A) RNA (1.5 µg) was reverse-transcribed at 37°C for 60 min in a 20 µl vol containing 1× reverse transcription buffer, 1 mM dNTPs, 400 U of superscript reverse transcriptase, 20 U of RNasin, and 20 pmol of oligo(dT)$_{12–18}$. The murine *WRN* sequence was amplified from the cDNA using PCR and the primers 5′-GATCAGCCCGGGGATGAGTGAAAAAAAATTGGA-3′ and 5′-GATCAGCTCGAGTCAAATTTGTTTCTGTTGTACTC-3′, and cloned into pFastBacHT to generate pBac-mN328. The cloned WRN sequences, exonuclease mutation and cloning in frame to the 6His tag in the expression vectors were verified by DNA sequencing.

Production, purification and analysis of recombinant proteins

Recombinant baculoviruses were produced according to the supplier's protocol. Transfer of the expression cassette into the viral genome was verified by PCR. Sf9 cells were cultured in suspension at 27°C. Cells (1–1.5 × 10^6/ml) were infected with recombinant viruses (m.o.i. = 3), and, 3 days later, collected by centrifugation, washed and stored at –80°C. For preparation of full-length protein, cells were lysed in 20 mM Tris–HCl, pH 7.2, 1% NP-40, 10% glycerol, 1 mM phenylmethylsulfonyl fluoride (PMSF), 10 µg/ml each of aprotinin and leupeptin. Nuclei were collected by centrifugation and resuspended in 20 mM Tris–HCl, pH 7.2, 0.4 M NaCl, 10% glycerol, 1 mM PMSF, 10 µg/ml each of aprotinin and leupeptin. The lysate was clarified by centrifugation and incubated with TALON resin at 4°C for 1 h. The resin was washed with 20 mM Tris–HCl, pH 7.2, 0.4 M NaCl, 25 mM imidazole, 10% glycerol, 1 mM PMSF, 10 µg/ml each of aprotinin and leupeptin, and proteins were eluted with 20 mM Tris–HCl, pH 7.2, 50 mM KCl, 500 mM imidazole (unless otherwise indicated), 10% glycerol, 10 µg/ml each of aprotinin and leupeptin. For preparation of N-terminal fragments, cytosolic lysates were clarified by centrifugation, adjusted to 400 mM NaCl, and subjected to TALON resin affinity purification as described above. Purified proteins were analyzed by denaturing sodium dodecyl sulfate–polyacrylamide gel electrophoresis (SDS–PAGE) and western blotting as described (23). Full-length protein was detected by immunoblotting using a rabbit polyclonal antibody against the C-terminal region of hWRN (20). N-terminal fragments were detected using a polyclonal antibody raised against hWRN amino acids 1–333.

Table 1. Oligonucleotides used to prepare nuclease substrates

Oligomer	Nucleotide sequence
23S	5′-d(CAGGCACAGGGTCAGGTCGGGGG)-3′
48A	5′-d(TTTTTTTTTTTTCCCCCCGACCTGACCCTGTGCCTGTTTTTTTTTTT)-3′
24S1	5′-d(CAGGCACAGGGTCAGGTCGGGGGG)-3′
24S2	5′-d(CTTGTCAGTCACTCAGAGCGTAGA)-3′
36S	5′-d(AAAAAAAAAAAACTTGTCAGTCACTCAGAGCGTAGA)-3′
18A	5′-d(GACCTGACCCTGTGCCTG)-3′
24A	5′-d(CCCCCCGACCTGACCCTGTGCCTG)-3′
60A1	5′-d(TCTACGCTCTGAGTGACTGACAAGTTTTTTTTTTTTCCCCCCGACC TGACCCTGTGCCTG)-3′
60A2	5′-d(TCTACGCTCTGAGTGACTGACAAGTTTTTTTTTTTT***G***CCCCCGACC TGACCCTGTGCCTG)-3′
60A3	5′-d(TCTACGCTCTGAGTGACTGACAAGTTTTTTTTTTTTCCCCCCGAC***T*** TGACCCTGTGCCTG)-3′
36A1	5′-d(TTTTTTTTTTTTCCCCCCGACCTGACCCTGTGCCTG)-3′
36A2	5′-d(TTTTTTTTTTTT***T***CCCCCGACCTGACCCTGTGCCTG)-3′
36A3	5′-d(TTTTTTTTTTTT***TT***CCCCGACCTGACCCTGTGCCTG)-3′
36A4	5′-d(TTTTTTTTTTTT***TTT***CCCGACCTGACCCTGTGCCTG)-3′
36A5	5′-d(TTTTTTTTTTTT***TTTTT***GACCTGACCCTGTGCCTG)-3′
30S	5′-d(GAGGAACACAGTCAGGTCACAGTCAAGGAG)-3′
30A1	5′-d(TTTTTTCTCCTTGACTGTGACCTGACTGTG)-3′
30A2	5′-d(CTCCTTGACTGTGACCTGACTGTGTTCCTC)-3′
30A3	5′-d(CTCCTTGACTGTGA***G***CTGACTGTGTTCCTC)-3′
30A4	5′-d(CTCCTTGACTGTG***GGGG***GACTGTGTTCCTC)-3′
25S	5′-d(GCTCGTAGTTGGATCTTGGGATAAG)-3′

Nuclease assays

Oligonucleotides used to make nuclease assay substrates are listed in Table 1. 5′ labeling was carried out using [γ-^{32}P]ATP and T4 polynucleotide kinase, whereas 3′ labeling was done using [α-^{32}P]dGTP and *E.coli* Klenow fragment. The substrates used in Figure 3 were prepared as follows. Oligonucleotide 24S1 was 5′ labeled and hybridized to 48A. The 3′ labeled substrate was prepared by labeling the 3′ end of the 23 nt strand of the prehybridized 23S/48A duplex. The substrates used in Figure 4 were prepared as follows. Oligonucleotide 24S1 was labeled at the 5′ end to make substrate 1. The labeled 24S1 was then hybridized to unlabeled 60A1, 18A, 24A, 36A1, 36A2, 36A3, 36A4 and 36A5 oligonucleotides to make substrates 2, 3, 4, 9, 10, 11, 12 and 13, respectively. The 5′ labeled 24S1 and unlabeled 24S2 were hybridized to unlabeled 60A1 to make substrate 5 (12 nt gap). The 5′ labeled 24S1 and unlabeled 36S were hybridized to unlabeled 60A1, 60A2 and 60A3 to make substrates 6, 7 and 8, respectively. 5′ labeled 30S was hybridized to unlabeled 30A1, 30A2, 30A3 and 30A4 to make substrates 14, 15, 16 and 17, respectively. 5′ labeled 25S was hybridized to a complementary RNA to make substrate 18. Hybridization was carried out in 10 mM Tris–HCl, pH 8.0 and 5 mM $MgCl_2$ using 1:3 molar ratios of labeled to unlabeled oligonucleotides for preparation of substrates 2–4 and 9–18, and 3:1 ratios of short to long oligonucleotides for preparation of substrates 5–8. Substrates were purified by 6–10% non-denaturing polyacrylamide gels and ethanol precipitation. The specific activities were ~5 × 10^6 c.p.m./pmol for

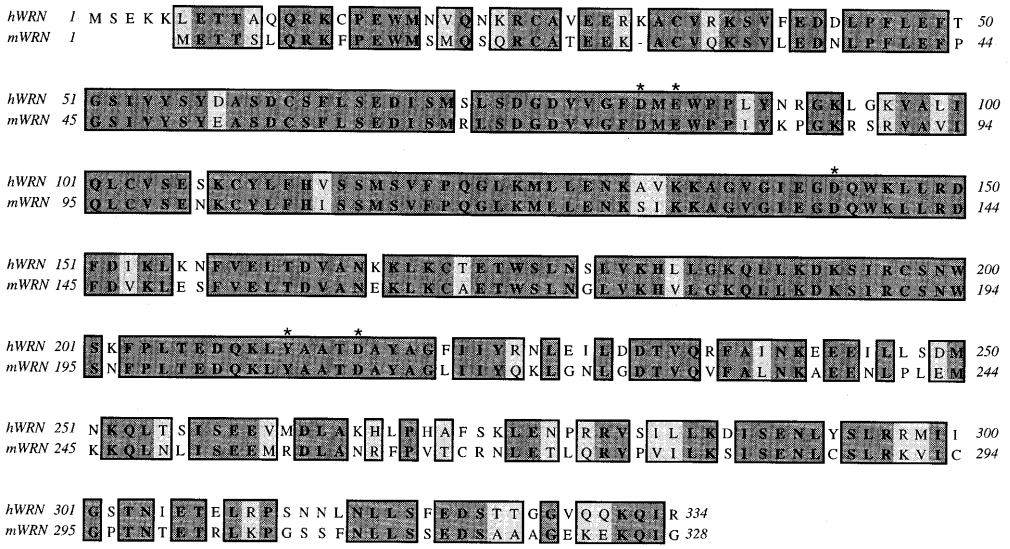

Figure 1. Amino acid sequence alignment of the N-terminal regions of hWRN and mWRN proteins. Identical amino acids are shaded in dark gray and similar amino acids in light gray. The five amino acids (D82, E84, D143, Y212 and D216 in human; D76, E84, D137, Y206 and D210 in mouse) critical for exonuclease activity are labeled with asterisks. The amino acid sequences were aligned using a MacVector software.

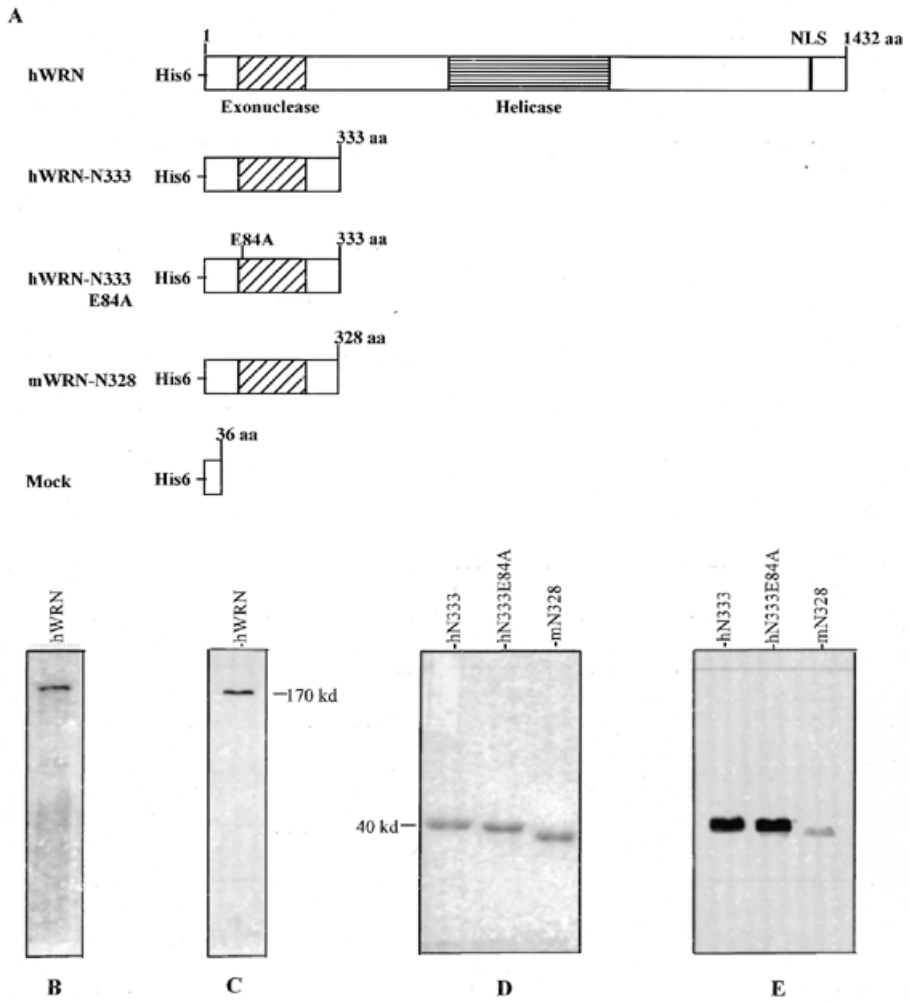

5′ labeled substrates and 2×10^6 c.p.m./pmol for 3′ labeled substrate. Nuclease assays was carried out in 20 µl as described (20). The reactions were terminated by adding 2 µl 100 mM EDTA, 22 µl loading dye (95% formamide, 0.025% xylene cyan, 0.025% bromphenol blue, 0.5 mM EDTA, 0.025% SDS), and heating at 95°C for 5 min. The products were analyzed on 20% polyacrylamide 1× TBE 8 M urea gels and visualized by autoradiography.

Oligomerization state of WRN

Ni (TALON)-affinity purified WRN (4 µg in 40 µl) and N333 (100 µg in 100 µl) were treated with 50 mM EDTA and 100 mM DTT for 15 min at 37°C and then subjected to gel filtration at 4°C by fast protein liquid chromatography. The columns were Superose 6 HR 10/30 for WRN and Superdex S-200 HR 10/30 for N333. The flow rate was 0.5 ml/min and fraction size was 1 ml for both columns. Proteins were eluted with 20 mM MOPS, pH 7.25, 0.5 M NaCl, 0.1 mM PMSF. The columns were calibrated using ovalbumin (43 kDa), bovine serum albumen (BSA, 67 kDa), aldolase (158 kDa), ferritin (440 kDa) and thyroglobulin (669 kDa). The protein in each elution fraction was concentrated by precipitation with 10% TCA in the presence of insulin (15 µg/ml) followed by washing and drying in acetone. The elution profiles of WRN and N333 were examined by SDS–PAGE and western blotting.

Interaction between WRN and PCNA

pGEX–GST–PCNA, containing the human PCNA cDNA fused to the GST coding sequence, was kindly provided by Dr Alan Tomkinson (University of Texas, San Antonio, TX). GST–TIN2 has been described (24). GST–PCNA and GST proteins were expressed in *E.coli* BL21, and purified by glutathione affinity chromatography using a commercial kit (Pharmacia). Proteins (1 µg) were immobilized on glutathione-Sepharose beads. The beads were washed with phosphate buffered saline (PBS), incubated for 1 h with 1 ml lysate from Sf9 cells infected with WRN or Mock (control) baculoviruses, washed with PBS and pelleted. Proteins were released from the beads by SDS–PAGE sample buffer at 95°C and analyzed by SDS–PAGE and western blotting. Alternatively, purified GST, GST–TIN2 or GST–PCNA (0.5 µg) were incubated with 0.5 µg purified recombinant WRN in 60 µl PBS for 1 h at 4°C, anti-GST (0.5 µg; Santa Cruz Biotechnology, Inc., Santa Cruz, CA) was added overnight at 4°C, and 25 µl of a 50% protein A-Sepharose slurry was added for 1 h. After washing with PBS, immune complexes were pelleted, resuspended in SDS–PAGE sample buffer and analyzed by SDS–PAGE and western blotting.

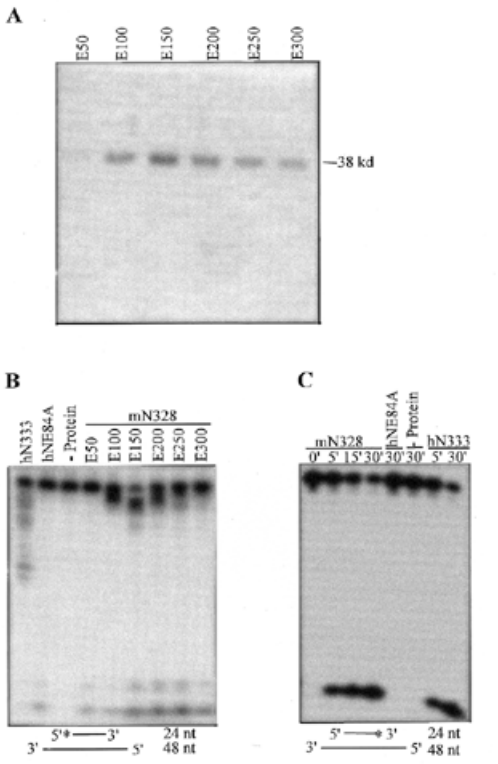

Figure 3. N-terminal region of mWRN is a 3′→5′ exonuclease. (**A**) mWRN-N328 was purified by Ni-affinity chromatography and eluted step-wise with increasing concentrations of imidazole as described in Materials and Methods. Equal volumes (10 µl) of each elution fraction (E) were analyzed by 12% SDS–PAGE stained with Coomassie blue. (**B**) Exonuclease activity of hWRN and mWRN N-terminal fragments using a 5′ labeled substrate shown below the autoradiogram. Equal volumes (1 µl) of each mWRN-N328 elution fraction were incubated with 20 000 c.p.m. of labeled substrate for 15 min. Controls were hWRN-N333 (20 ng), hWRN-N333E84A (20 ng) and reaction lacking protein. The protein inputs of mWRN-N328 fractions varied between 5 (E50) and 100 ng (E150). (**C**) Exonuclease activity of hWRN and mWRN N-terminal fragments using a 3′ labeled substrate shown below the autoradiogram. Proteins (20 ng hWRN-N333 and hWRN-N333E84; 100 ng mWRN-N328) were incubated with substrate for the indicated intervals. Reaction products were analyzed by 20% PAGE as described in Materials and Methods.

RESULTS

Cloning and characterization of the mWRN N-terminal region

The hWRN exonuclease domain lies within the first 333 amino acids of the protein (18–20). Because human and mouse *WRN* cDNAs encode similar proteins (13,25), it was likely that the

Figure 2. (Opposite) Analysis of affinity-purified recombinant WRN proteins. (**A**) Diagram of the constructs used to produce the recombinant WRN proteins. hWRN, fulllength wild-type human protein; hWRN-N333, human N-terminal WRN fragment containing amino acids 1–333; hWRN-N333E84A, human N-terminal WRN fragment exonuclease mutant harboring a point mutation from Glu (E) to Ala (A) at amino acid 84; mWRN-N328, mouse N-terminal WRN fragment containing amino acids 1–328. The exonuclease domain is designated by a hatched box and the helicase domain by a box with horizontal bars. NLS, nuclear localization signal. (**B** and **C**) Full-length human wild-type WRN. Wild-type hWRN (1 µg) was analyzed by 10% SDS–PAGE stained with Coomassie brilliant blue (B) and western blotting using a polyclonal antibody against the hWRN C-terminal region (C). (**D** and **E**) N-terminal WRN fragments. hWRN-N333, hWRN-N333E84A and mWRN-N328 proteins (2 µg each) were analyzed by 12% SDS–PAGE stained with Coomassie brilliant blue (D) and western blotting using a polyclonal antibody against the hWRN N-terminal region (E).

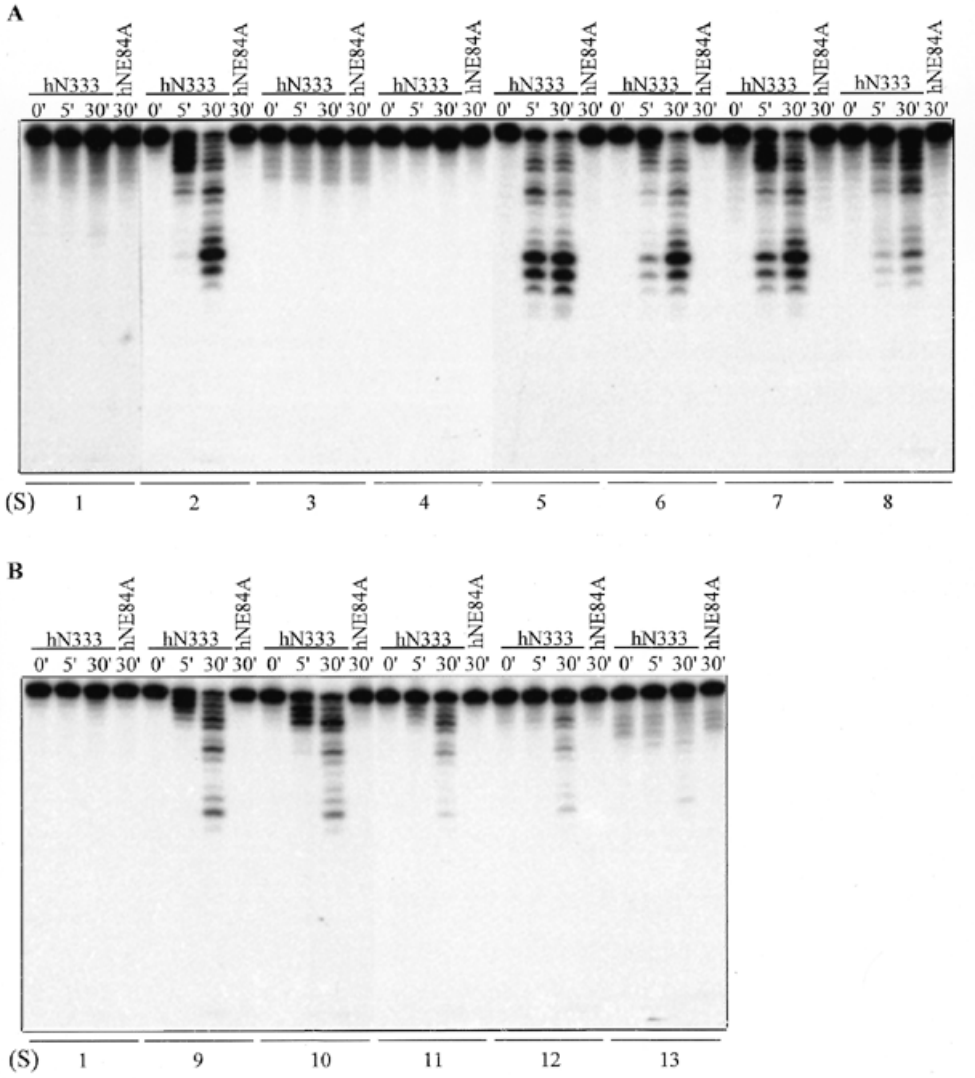

mWRN N-terminal region also had intrinsic exonuclease activity. However, this prediction had not been confirmed. On the other hand, the short life span of mice, and their resistance to some pathologies that are prevalent in WS (e.g., cardiovascular disease), raised the possibility that mWRN and hWRN differ in one or more activity.

To determine whether mWRN is also an exonuclease, we cloned the cDNA encoding the N-terminal mWRN region (amino acids 1–328, corresponding to 1–333 of hWRN). Sequence analysis showed that the cloned cDNA was essentially identical to the mWRN cDNA sequence in the GenBank database, with only three nucleotide substitutions, which may be polymorphisms (data not shown). The amino acid sequence encoded by the cloned mWRN cDNA is aligned with the N-terminal region of hWRN in Figure 1. The mouse sequence is highly homologous to the human sequence, with ~70% amino acid identity. The identical amino acids include all five amino acids (D76, E78, D137, Y206 and D210 in the mouse sequence) predicted to be critical for hWRN exonuclease activity (18,19).

Purification of full-length WRN and N-terminal WRN fragments

cDNAs encoding full-length (hWRN) or N-terminal (hWRN-N333, hWRN-N333E84A, mWRN-N328) proteins were cloned into a baculoviral expression vector (Fig. 2A). A point mutation from Glu→Ala at amino acid 84 (E84A), previously shown to obliterate exonuclease activity of full-length hWRN (20), was introduced into the N-terminal fragment. The recombinant proteins were expressed in baculovirus-infected insect cells, and purified by Ni-affinity chromatography. Purified full-length hWRN had an apparent molecular weight of ~170 kDa (Fig. 2B), as expected from the calculated molecular weight and additional N-terminal 36 amino acids encoded by the 6His tag and vector. Western analysis of the purified protein, using an antibody raised against the hWRN C-terminus, showed a single band of the appropriate molecular size (Fig. 2C). Purified hWRN-N333 and hWRN-N333E84A had apparent molecular weights of 40 kDa (Fig. 2D), and purified mWRN-N328 had

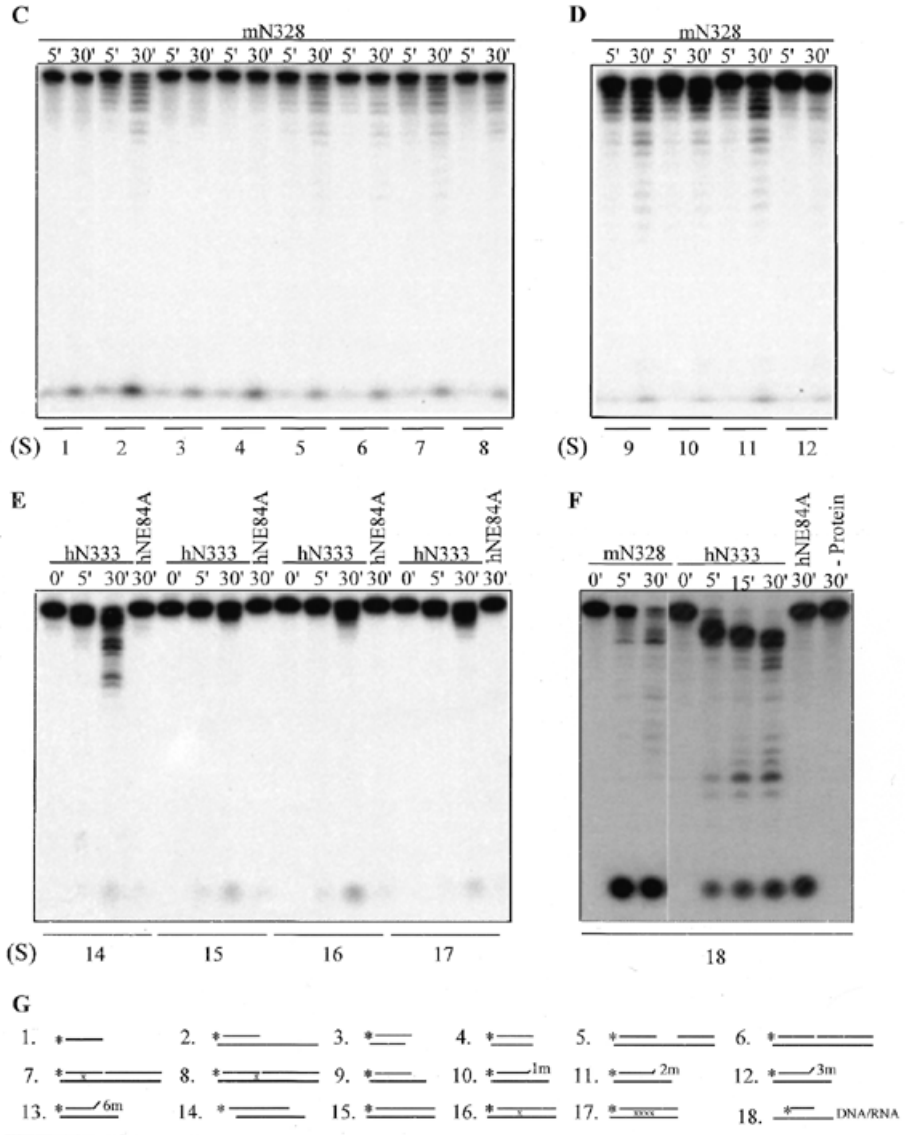

Figure 4. (Opposite and above) Substrate preferences of hWRN and mWRN 3′→5′ exonucleases. (**A**–**F**) Proteins (20 ng hWRN-N333 and hWRN-N333E84A, 100 ng mWRN-N328) were incubated with 20 000 c.p.m. of 5′ labeled substrates (S) shown below the autoradiogram for the indicated intervals. Reaction products were analyzed as described in Materials and Methods. (**G**) X shown on the substrates indicates mismatched base pairs. 1m, 2m, 3m and 6m indicate 1, 2, 3 and 6 mismatched nucleotides, respectively.

an apparent molecular weigh of 38 kDa, also consistent with the calculated molecular weights and additional vector sequence. A polyclonal antibody raised against the hWRN N-terminus clearly detected purified hWRN N-terminal fragments as single bands in western analyses (Fig. 2E). The antibody also detected the purified mWRN N-terminal fragment, although reactivity was less robust (Fig. 2E).

The N-terminal region of mWRN contains 3′→5′ exonuclease activity

The hWRN exonuclease activity resides in the first 333 amino acids of the protein (20). The corresponding region (amino acids 1–328) of mWRN also showed 3′→5′ exonuclease activity when assayed using 5′ and 3′ labeled DNA substrates (Fig. 3). mWRN-N328 was eluted step-wise from the Ni-affinity column using increasing imidazole concentrations (50–300 mM), with peak elution occurring at 150 mM (Fig. 3A). Equal volumes of these protein fractions were assayed for exonuclease activity. Like hWRN-N333, mWRN-N328 degraded a 5′ labeled substrate into a series of smaller labeled products (Fig. 3B). The amount of degradation correlated well with the concentration of mWRN-N328 in the fractions. When incubated with a 3′ labeled DNA substrate, mWRN-N328 produced only a single labeled product that migrated as a mononucleotide, as observed for

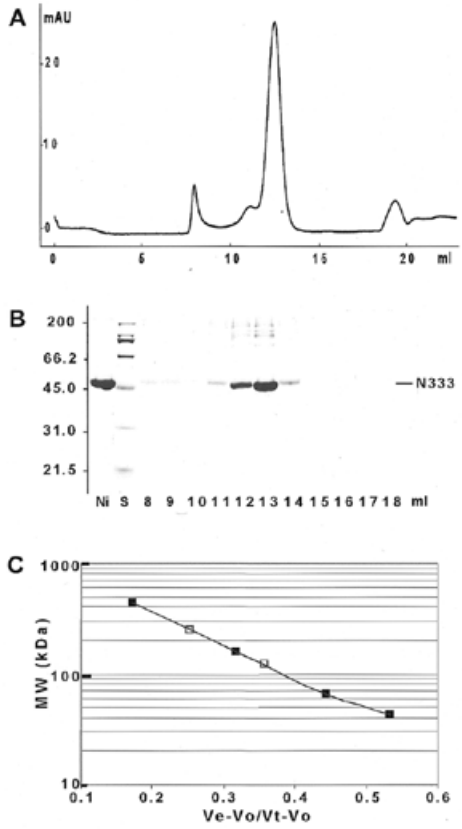

Figure 5. Analysis of quaternary structure of recombinant hWRN-N333 by gel filtration chromatography. (**A**) Elution profile of Superdex S-200 HR 10/30 column. (**B**) 12% SDS–PAGE analysis of eluted proteins. The gel was stained with Coomassie blue. Ni, hWRN-N333-containing fraction from the Ni-TALON column; S, SDS–PAGE molecular weight standards. (**C**) Elution of the hWRN-N333 oligomers and molecular weight markers on Superdex S-200 chromatography. The molecular weight markers were ferritin (440 kDa), aldolase (158 kDa), BSA (67 kDa) and ovalbumin (43 kDa). The first elution peak from the column was considered the exclusion volume (Vo). Vt was determined by the elution of salt from the column. Ve is the elution volume of hWRN-N333 oligomers (open squares) and molecular weight markers (closed squares).

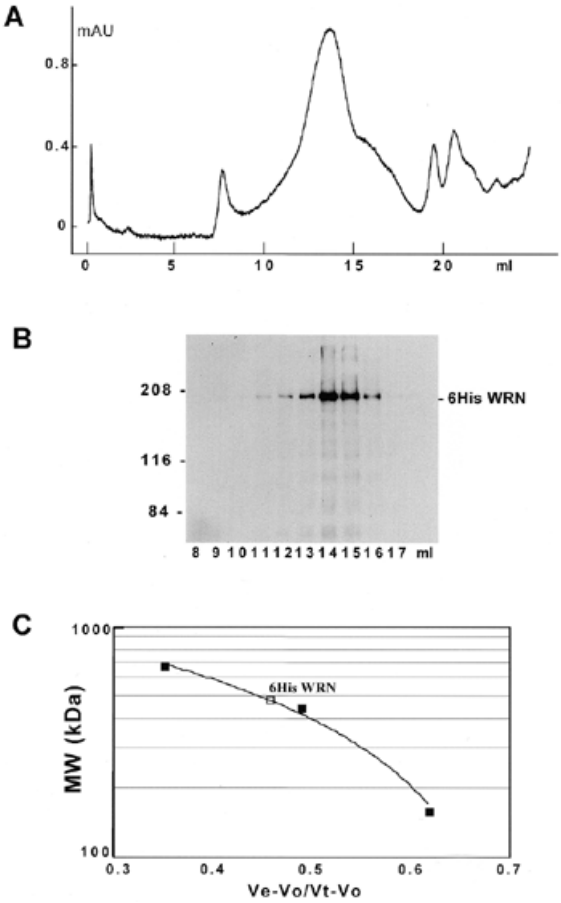

Figure 6. Analysis of quaternary structure of recombinant hWRN by gel filtration chromatography. (**A**) Elution profile of Superose 6 HR 10/30 column. (**B**) 6% SDS–PAGE analysis of eluted proteins. The gel was analyzed by western blotting using a polyclonal antibody against the hWRN C-terminal region. (**C**) Calibration of the WRN oligomers and the molecular weight markers on Superose 6 chromatography. The molecular weight markers utilized were thyroglobulin (669 kDa), ferritin (440 kDa) and aldolase (158 kDa). Vo, Vt and Ve were determined as described in the legend to Figure 5.

hWRN-N333 (Fig. 3C; 20). The exonuclease mutant hWRN-N333E84A showed no such activity on either 5′ or 3′ labeled substrates. The fastest migrating product in reactions with the 5′ labeled substrate was due to a small amount of contaminating 5′→3′ activity from the insect cells; this product was also observed in reactions using the exonuclease mutant hWRN-N333E84A (Fig. 3B), and identically purified proteins from cells infected with a control virus (containing no WRN sequences) (data not shown). These data indicate that both the hWRN and mWRN proteins are 3′→5′ exonucleases.

hWRN and mWRN exonucleases display similar substrate specificities

The hWRN and mWRN exonucleases were assayed using 18 different substrates (Fig. 4). Both exonucleases greatly preferred double-stranded DNA with a 5′ overhang over blunt-ended DNA, double-stranded DNA with a 3′ overhang, or single-stranded DNA (Fig. 4A and C, substrates 1–4). Interestingly, the exonucleases also acted on double-stranded DNA containing a gap or nick (Fig. 4A and C, substrates 5–8). Both proteins were as active on nicked or gapped substrates as on DNA duplexes with a 5′ overhang. Introduction of a single mismatch at the 3′ terminus, or at the 3′ end of a nick had little effect on hWRN or mWRN exonuclease activities. Both exonucleases efficiently removed one terminal mismatched nucleotide (Fig. 4B and D, compare activity on substrates 10 and 11 to that on substrate 9). However, as the number of terminal mismatches increased, activity decreased (Fig. 4B and D, substrate 12). When the number of terminal mismatched nucleotides was increased to six, essentially no activity was detected for both the human (Fig. 4B, substrate 13) and mouse proteins (data not shown).

hWRN-N333 displayed no endonuclease activity. When tested on double-stranded DNA with blunt ends or a 3′ overhang, or single-stranded DNA, it did not cleave at internal sites (Fig. 4, substrates 1, 3, 4 and 15). Furthermore, when tested on blunt-ended double-stranded DNA containing one or four internal mismatches, no endonuclease activity was detected (Fig. 4, substrates 16 and 17). Similar results were obtained with mWRN-N328 (not shown). Finally, WRN was capable of degrading a DNA–RNA hybrid. Both hWRN-N333 and mWRN-N328 degraded the DNA strand of a DNA–RNA duplex containing recessed 3′ and 5′ ends (Fig. 4F). The fastest migrating degradation product in all the lanes, but most evident in those containing the DNA–RNA substrate (Fig. 4F), is likely due to a contaminating 5′→3′ exonuclease, because it is produced independent of the WRN exonuclease (hNE84A mutant lane). This minor contaminant, which we have noted previously (20), appears to be much more active on the DNA–RNA substrate relative to the other substrates.

hWRN forms a trimer *in vitro*

To determine the quaternary structure of WRN, we employed gel filtration chromatography of the recombinant proteins. Purified recombinant hWRN-N333 was applied to a Superdex S-200 column. Most of the protein (>90%) eluted in a peak corresponding to a molecular mass of 130 kDa (Fig. 5, fractions 12 and 13). A small amount (<10%) of higher molecular material was present in fractions 12 and 13, but these were absent from the starting material (fraction Ni), and appeared to be generated by the TCA precipitation used to concentrate the fractions. Because the predicted mass of the recombinant hWRN-N333 protein is ~42 kDa, the oligomerization state of the protein appears to be a trimer. A minor fraction of hWRN-N333 eluted in a peak corresponding to a mass of 250 kDa, consistent with a hexameric oligomerization state. We also assessed the oligomerization status of full-length WRN. Recombinant full-length hWRN was applied to a Superose 6 column. Most of the protein eluted in a peak corresponding to a molecular mass of 465 kDa (Fig. 6). Because the predicted mass of the recombinant full-length WRN is 165 kDa, the oligomerization state of full-length hWRN also appeared to be a trimer. Thus, the quaternary structure of WRN appears to differ from that of BLM, which was reported to be hexameric (26).

hWRN interaction with PCNA

Because WRN may be involved in DNA replication and/or repair (Discussion), we asked whether WRN interacted with proteins known to participate in these processes. In agreement with a recent report (27), WRN interacted with one such protein, the PCNA (Fig. 7). Recombinant GST or a GST–PCNA fusion protein was immobilized on glutathione-Sepharose beads, and incubated with lysates from insect cells infected with hWRN- or Mock (control)-expressing baculoviruses. Proteins specifically bound to the beads were released and analyzed by western blotting. WRN bound to GST–PCNA, but not GST (Fig. 7B). Alternatively, purified recombinant hWRN was incubated with GST–PCNA, GST or GST–TIN2, a telomere binding protein (24) used to demonstrate specificity. Complexes immunoprecipitated by anti-GST were analyzed by western blotting (Fig. 7C). WRN was present in complexes containing GST–PCNA, but not GST or GST–TIN2. Taken together, these data suggest that WRN is capable

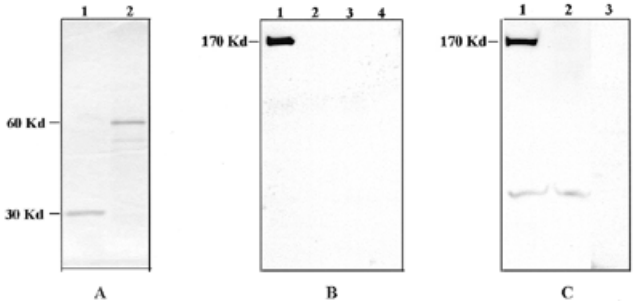

Figure 7. Interaction between WRN and PCNA proteins. (**A**) SDS–PAGE analysis of purified recombinant GST and GST–PCNA proteins. The glutathione-affinity purified proteins (1 μg each) were resolved on a 12% SDS–PAGE gel and stained with Coomassie blue. The approximate sizes of the proteins (GST, 30 kDa; GST–PCNA, 60 kDa) are indicated. (**B**) WRN–PCNA interaction detected by affinity chromatography. Glutathione-Sepharose beads containing 1 μg immobilized GST–PCNA (lanes 1 and 3) or GST (lanes 2 and 4) were used to pull down proteins from1 ml lysate prepared from insect cells infected with a WRN (lanes 1 and 2) or a Mock (lanes 3 and 4) recombinant baculovirus, as described in Materials and Methods. The interacting proteins were resolved by 10% SDS–PAGE and analyzed by western blotting using an anti-WRN antibody. (**C**) WRN–PCNA interaction detected by co-immunoprecipitation. WRN (0.5 μg) protein was incubated with 0.5 μg of GST–PCNA (lane 1), GST (lane 2) or GST–TIN2 (lane 3) protein and immunoprecipitated using an anti-GST antibody. The precipitated proteins were resolved by 10% SDS–PAGE, and analyzed by western blotting.

of interacting with PCNA *in vitro*, at least under these conditions, and that the interaction is direct. Whether and under what circumstances this interaction occurs *in vivo*, is not known at this time. Before we completed a full characterization of this interaction, a report was published showing that WRN interacts with PCNA *in vitro* and in nuclear replication complexes (27).

DISCUSSION

WRN belongs to the RECQ helicase family whose members include *E.coli* RECQ, *Saccharomyces cerevisiae* SGS1, and human RECQL, BLM, WRN, RECQL4 and RECQL5. WRN is unique among these helicases in that it is also an exonuclease (18–21). This activity, which hydrolyzes double-stranded DNA with 3′→5′ directionality, is located in the N-terminal region of the protein.

We cloned and expressed the N-terminal region of the mouse WRN protein, and showed that it is also an exonuclease with 3′→5′ polarity. The substrate specificity of mWRN was markedly similar to that of hWRN. The only difference we observed between the hWRN and mWRN exonucleases was that the mouse protein appeared to be somewhat less active than the human protein. The N-terminal region of mWRN is 30% divergent from the corresponding region of hWRN. This sequence divergence could be responsible for the reduced activity of the mWRN exonuclease. Alternatively, the mWRN exonuclease may have slightly different salt, pH or other requirements for optimal activity. Recently, exonuclease activity with the opposite polarity (5′→3′) was reported for hWRN (28). We (20) and others (21) have not observed 5′→3′ activity intrinsic to WRN.

In this study, the N-terminal fragments were purified to >90% homogeneity, and both the human and mouse fragments showed 3′→5′ exonuclease activity. We introduced a Glu→Ala substitution at amino acid 84 in the human fragment. This residue is one of five predicted to be critical for exonuclease activity (18,19). The mutation abolished the 3′→5′ exonuclease activity of the fragment, as it did in the full-length protein (20). An independent point mutation (D82A, Asp→Ala at amino acid 82) also inactivated the 3′→5′ exonuclease activity of full-length hWRN (20). Thus, biochemical and genetic data indicate that WRN is a 3′→5′ exonuclease. Moreover, this activity exists in both the human and mouse proteins.

Despite slightly different levels of activity, the hWRN and mWRN exonucleases displayed strikingly similar substrate specificities. First, both enzymes preferred a 3′ recessed terminus. Little or no activity was observed on blunt-ended double-stranded DNA, or a protruding 3′ strand. Similarly, little activity was observed on single-stranded DNA. Second, both enzymes were capable of removing a terminal mismatched nucleotide as efficiently as they removed a terminal matched nucleotide. However, the efficiency of terminal nucleotide removal decreased dramatically as the number of mismatches increased. The enzyme was barely active on a DNA duplex with three terminal mismatches, and no activity was detected on a duplex with six terminal mismatches. Third, both enzymes were capable of initiating degradation from gapped or nicked double-stranded DNA. Finally, neither the mouse nor human N-terminal fragments displayed endonuclease activity on blunt-ended substrates, suggesting that they are devoid of endonuclease activity. Identical substrate specificities were observed for full-length hWRN (not shown), suggesting that the N-terminal fragments contained all the amino acids needed for exonuclease activity. The substrate preferences of the WRN exonuclease are similar to those of *E.coli* exo III (29). However, unlike exo III, WRN has no endonuclease activity. One difference between the mWRN and hWRN exonucleases is the degradation pattern of the 5′ labeled substrates, which could indicate a difference in processivity between the two enzymes.

We do not as yet know the exact function(s) of the WRN exonuclease (or helicase) *in vivo*. One possibility is that WRN participates in one or more aspect of DNA replication, since abnormalities in S phase initiation or transit have been reported (6,30). The efficient removal of a terminal mismatched nucleotide raises the possibility that WRN may provide 3′→5′ proofreading activity for DNA polymerases that lack such activity. WS cells are known to be hypermutable (9,10,31), accumulating cytogenetic abnormalities consistent with deletions and rearrangements. However, it is not known whether WS cells also accumulate point mutations. WRN is homologous to FFA-1, a *Xenopus laevis* protein required for replication focus formation during DNA replication (32). Finally, the findings that WRN interacts with PCNA, and is associated with a mammalian DNA replication complex (27), suggest that WRN may function in DNA replication.

The WRN exonuclease may also function in DNA repair, since PCNA also functions in DNA repair, and WRN can initiate DNA degradation from a nick. Mismatch repair involves an incision on the damaged DNA strand followed by removal by an exonuclease (33). WRN can potentially fulfill the exonuclease requirement in this process. However, evidence for a deficiency in mismatch repair in WS is limited. Such a deficiency was reported for SV40-transformed WS cells (34), but the repair deficiency could not be unambiguously attributed to a defect in WRN. However, WRN may participate in the repair of other types of DNA damage. WS cells are hypersensitive to 4NQO, which leads to elevated rates of chromosome breaks and exchanges (35). This hypersensitivity suggests that WRN may participate in the repair of such damage. Finally, the homology to RECQ suggests that the WRN exonuclease, together with the WRN or another helicase, may act in a recombinational pathway, which can repair double strand DNA breaks.

Most helicases characterized to date form either dimers or hexamers (36). For example, *E.coli* UvrD is dimeric (37) and BLM is hexameric (26). Interestingly, recombinant hWRN eluted as a trimer in gel filtration assays. The oligomerization state of WRN could be important for its function. The human genome encodes more than 30 helicases, a number that may increase upon complete characterization of the genome (16). Thus far, five are members of the RECQ family, and three of these are associated with hereditary disorders (13,17,38–40). In addition to WS, defects in BLM cause Bloom's syndrome (41), and defects in RECQL4 cause a subset of Rothmund–Thomson syndrome (42). All three syndromes are cancer-prone, but differ markedly in other associated pathophysiology. Differential expression may contribute to the distinct phenotypes caused by defects in these helicases (17). Our finding that hWRN forms trimers, in contrast to the ability of BLM to form hexamers, suggests another level of distinction between these helicases. Although oligomerization of a helicase may not be essential for activity (43), oligomeric structure may influence substrate specificity and/or ability to interact with different regulatory proteins, and thus lead to different functions. It is interesting, therefore, that WRN interacts with PCNA, which also forms trimers (44). The trimerization of WRN and PCNA may not be a coincidence. WRN trimers may provide the necessary quaternary structure for interaction with trimeric PCNA. Such an interaction might enhance WRN exonuclease and/or helicase activities, possibilities that remain to be explored in future studies.

ACKNOWLEDGEMENTS

This work was supported by grants from the National Institute on Aging, AG05776 (S.H.) and AG11658 (J.C.), under Department of Energy contract DE-AC0376SF00098 to the University of California, and AG14446 (J.O.). N.A.E. and S.B. were supported by the Sloan-Kettering Institute and May and Samuel Rudin Family Foundation, Inc.

REFERENCES

1. Martin,G.M. (1978) *Birth Defects*, **14**, 5–39.
2. Goto,M. (1997) *Mech. Ageing Dev.*, **98**, 239–254.
3. Martin,G.M., Oshima,J., Gray,M.D. and Poot,M. (1999) *J. Am. Geriatr. Soc.*, **47**, 1136–1144.
4. Martin,G.M., Sprague,C.A. and Epstein,C.J. (1970) *Lab. Invest.*, **23**, 86–92.
5. Salk,D., Bryant,E., Hoehn,H., Johnston,P. and Martin,G.M. (1985) *Adv. Exp. Bio. Med.*, **190**, 305–311.
6. Poot,M., Hoehn,H., Runger,T.M. and Martin,G.M. (1992) *Exp. Cell Res.*, **202**, 267–273.
7. Schulz,V., Zakian,V.A., Ogburn,C.E., McKay,J., Jarzebowicz,A.A., Edland,S.D. and Martin,G.M. (1996) *Hum. Genet.*, **97**, 750–754.

8. Oshima,J., Campisi,J., Tannock,T.C., Sybert,V.P. and Martin,G.M. (1995) *J. Cell Physiol.*, **162**, 277–283.
9. Salk,D., Au,K., Hoehn,H. and Martin,G.M. (1981) *Cytogenet. Cell Genet.*, **30**, 92–107.
10. Fukuchi,K., Martin,G.M. and Monnat,R.J. (1989) *Proc. Natl Acad. Sci. USA*, **86**, 5893–5897.
11. Cheng,R.Z., Murano,S., Kurz,B. and Shmookler-Reis,R.J. (1990) *Mutat. Res.*, **237**, 259–269.
12. Ogburn,C.E., Oshima,J., Poot,M., Chen,R., Hunt,K.E., Gollahon,K.A., Rabinovitch,P.S. and Martin,G.M. (1997) *Hum. Genet.*, **101**, 121–125.
13. Yu,C.E., Oshima,J., Fu,Y.H., Wijsman,E.M., Hisama,F., Alisch,R., Matthews,S., Nakura,J., Miki,T., Ouais,S., Martin,G.M., Mulligan,J. and Schellenberg,G.D. (1996) *Science*, **272**, 258–262.
14. Gray,M.D., Shen,J.C., Kamath-Loeb,A.S., Blank,A., Sopher,B.L., Martin,G.M., Oshima,J. and Loeb,L.A. (1997) *Nature Genet.*, **17**, 100–103.
15. Suzuki,N., Shimamoto,A., Imamura,O., Kuromitsu,J., Kitao,S., Goto,M. and Furuichi,Y. (1997) *Nucleic Acids Res.*, **25**, 2973–2978.
16. Ellis,N.A. (1997) *Curr. Opin. Genet. Dev.*, **7**, 354–363.
17. Kitao,S., Ohsugi,I., Ichikawa,K., Goto,M., Furuichi,Y. and Shimamoto,A. (1998) *Genomics*, **54**, 443–452.
18. Moser,M.J., Holley,W.R., Chatterjee,A. and Main,I.S. (1997) *Nucleic Acids Res.*, **25**, 5110–5118.
19. Mushegian,A.R., Bassett,D.E.,Jr, Boguski,M.S., Bork,P. and Koonin,E.V. (1997) *Proc. Natl Acad. Sci. USA*, **94**, 5831–5836.
20. Huang,S., Li,B., Gray,M.D., Oshima,J., Mian,S. and Campisi,J. (1998) *Nature Genet.*, **20**, 114–116.
21. Shen,J.-C., Gray,M.D., Oshima,J., Kamath-Loeb,A.S., Fry,M. and Loeb,L.A. (1998) *J. Biol. Chem.*, **273**, 34139–34144.
22. Ho,S.N., Hunt,H.D., Horton,R.M., Pullen,J.K. and Prase,L.R. (1989) *Gene*, **77**, 51–59.
23. Ausubel,F., Brent,B., Kingston,R.E., Moore,D.D., Seidman,J.G., Smith,J.A. and Struhl,K. (1994) *Current Protocols in Molecular Biology*. John Wiley & Sons, Inc., New York, NY.
24. Kim,S.H., Kaminker,P. and Campisi,J. (2000) *Nature Genet.*, **23**, 405–412.
25. Imamura,O., Ichikawa,K., Yamabe,Y., Goto,M., Sugawara,M. and Furuichi,Y. (1997) *Genomics*, **41**, 298–300.
26. Karow,J.K., Newman,R.H., Freemont,P.S. and Hickson,I.D. (1999) *Curr. Biol.*, **9**, 597–600.
27. Lebel,M., Spillare,E.A., Harris,C.C. and Leder,P. (1999) *J. Biol. Chem.*, **274**, 37795–37799.
28. Suzuki,N., Shiratori,M., Goto,M. and Furuichi,Y. (1999) *Nucleic Acids Res.*, **27**, 2361–2368.
29. Kornberg,A. and Baker,T.A. (1992) *DNA Replication*. 2nd Edn. W.H. Freeman and Co., New York, NY.
30. Takeuchi,F., Hanaoka,F., Goto,M., Akaoka,I., Hori,T.-A., Yamada,M.-A. and Miyamoto,T. (1982) *Hum. Genet.*, **60**, 365–368.
31. Fukuchi,K.-I., Tanaka,K., Nakura,J., Kumahara,Y., Uchida,T. and Okada,Y. (1985) *Somatic Cell Mol. Genet.*, **11**, 303–308.
32. Yan,H., Chen,C.-Y., Kobayashi,R. and Newport,J. (1998) *Nature Genet.*, **19**, 375–378.
33. Modrich,P. (1994) *Science*, **266**, 1959–1960.
34. Bennett,S.E., Umar,A., Oshima,J., Monnat,R.J. and Kunkel,T.A. (1997) *Cancer Res.*, **57**, 2956–2960.
35. Gebhart,E., Bauer,R., Schinzel,M., Ruprecht,K.W. and Jones,J.B. (1980) *Hum. Genet.*, **80**, 135–139.
36. Lohman,T.M. and Bjornson,K.P. (1996) *Annu. Rev. Biochem.*, **65**, 169–214.
37. Runyon,G.T., Wong,I. and Lohman,T.M. (1993) *Biochemistry*, **32**, 602–612.
38. Puranam,K.L. and Blackshear,P.J. (1994) *J. Biol. Chem.*, **269**, 29838–29845.
39. Seki,M., Miyazawa,H., Tada,S., Yanagiswawa,J., Yamaoka,T., Hoshino,S., Ozawa,K., Eki,T., Nogami,M., Okumura,K., Taguchi,H., Hanaoka,F. and Enomoto,T. (1994) *Nucleic Acids Res.*, **22**, 4566–4573.
40. Ellis,N.A., Groden,J., Ye,T.Z., Straughen,J., Lennon,D.J., Ciocci,S., Proytcheva,M. and German,J. (1995) *Cell*, **83**, 655–666.
41. German,J. (1993) *Medicine*, **72**, 393–406.
42. Kitao,S., Shimamoto,A., Goto,M., Miller,R.W., Smithson,W.A., Lindor,N.M. and Furuichi,Y. (1999) *Nature Genet.*, **22**, 82–84.
43. Mechanic,L.E., Hall,M.C. and Matson,S.W. (1999) *J. Biol. Chem.*, **274**, 12488–12498.
44. Krishna,T., Kong,X., Gray,S., Burgers,P. and Kuriyan,J. (1994) *Cell*, **79**, 1233–1243.